University of Baghdad
College of Engineering
JOURNAL OF ENGINEERING

Journal of Engineering

journal homepage: www.joe.uobaghdad.edu.iq
Number 10 Volume 24 October 2018

Chemical, Petroleum and Environmental Engineering

Synthesis and Characterization of Magnetic Iron Oxide Nanoparticles by Co-Precipitation Method at Different Conditions

Ahmed Faiq Al-Alawy*
Professor
College of Engineering-University of Baghdad
ahmedalalawy@yahoo.com

Entisar Eliwi Al-Abodi
Assistant Professor
College of Education Ibn Al-Haitham-University of Baghdad
entisaree2000@gmail.com

Raya Mohammed Kadhim
Senior engineer
Ministry of health and environment-Department of International Environment Relationships
chengraya@yahoo.com

ABSTRACT

Magnetic nanoparticles (MNPs) of iron oxide (Fe_3O_4) represent the most promising materials in many applications. MNPs have been synthesized by co-precipitation of ferric and ferrous ions in alkaline solution. Two methods of synthesis were conducted with different parameters, such as temperature (25 and 80℃), adding a base to the reactants and the opposite process, and using nitrogen as an inert gas. The product of the first method (MNPs-1) and the second method (MNPs-2) were characterized by x-ray diffractometer (XRD), Zeta Potential, atomic force microscope (AFM) and scanning electron microscope (SEM). AFM results showed convergent particle size of (MNPs-1) and (MNPs-2) with (86.01) and (74.14) nm respectively. Also, the zeta potential values of (MNPs-1) and (MNPs-2) were (2.77) and (-12.48) mV, respectively, which indicates more stability of (MNP-2).

Key Words: magnetic nanoparticles, iron oxide, co-precipitation.

تصنيع وتشخيص دقائق أوكسيد الحديد النانوية المغناطيسية بطريقة الترسيب المشترك عند ظروف مختلفة

أحمد فائق العلوي
أستاذ
كلية الهندسة-جامعة بغداد

انتصار عليوي العبودي
استاذ مساعد
كلية التربية ابن الهيثم-جامعة بغداد

ريا محمد كاظم
مهندس اقدم
وزارة الصحة والبيئة-قسم علاقات البيئة الدولية

الخلاصة

الدقائق النانوية المغناطيسية (MNPs) لأوكسيد الحديد (Fe_3O_4) تمثل أكثر المواد الواعدة في العديد من التطبيقات. تم تصنيع الدقائق النانوية المغناطيسية بطريقة الترسيب المشترك لأيونات الحديديك والحديدوز في محلول قلوي. تم إتباع طريقتين للتصنيع وبعوامل مختلفة، مثل الحرارة (25 و 80 °م)، إضافة القاعدة الى المواد المتفاعلة والعملية العكسية لها، و إستخدام النتروجين كغاز خامل. تم تشخيص ناتج الطريقة الأولى (MNPs-1) والطريقة الثانية (MNPs-2) بواسطة جهاز حيود الأشعة السينية (XRD)

*Corresponding author
Peer review under the responsibility of University of Baghdad.
https://doi.org/10.31026/j.eng.2018.10.05

Article accepted: 16/11/2017

وجهد زيتا ومجهر القوى الذرية (AFM) والمجهر الألكتروني الماسح (SEM). نتائج فحص AFM بينت تقارب في حجم دقائق (MNPs-1) و (MNPs-2) بقيمة (86,01) و (74,14) نانومتر، على التوالي. كذلك قيم جهد زيتا لـ (MNPs-1) و(MNPs-2) كانت (2,77) و(- 12,48) ملي فولت، على التوالي، والذي يعد مؤشراً على أن (MNPs-2) أكثر استقراراً من (MNPs-1).

الكلمات الرئيسية: دقائق نانوية مغناطيسية ، أوكسيد الحديد، الترسيب المشترك.

1. INTRODUCTION

Nanoscience is one of the most important recent research areas, **Mahdavi, et al., 2013**. It is now broadly used in the medicine, pharmaceutical manufacturing, engineering, electronics, robotics, material science and environmental areas, **Hyeon, 2003**. Due to their exceptional size and physical properties, the use of nanoparticle (NP) materials proposes various benefits, **Faraji, et al., 2010**. For over a decade, the synthesis of transition metals and their oxide NPs has been an area of intensive study because of their perspective and practical applications in cancer therapy, water treatment, magnetic fluid separation, heat transfer enhancement, adsorption, and so on, **Hong, et al., 2008**. Magnetite (Fe_3O_4) is a widespread magnetic iron oxide. It has an inverse (cubic) spinel structure with oxygen (anions) creating a face-centered cubic (fcc) closed packing and iron (cations) located at the interstitial tetrahedral sites (T_d) and octahedral sites (O_h), **Cornell, and Schwertmann, 1996**. Magnetite NPs have earned a lot of attention in many applications due to specific characteristics for each application. In biomedical applications, such as drug delivery and magnetic resonance imaging (MRI), and in industrial applications, MNPs are used due to their biocompatibility, low toxicity, ease of surface modification, magnetic properties, and chemical stability, **Bucak, et al., 2012.** In the field of information storage and magnetic sensing, they are used due to the strong need for high-density storage, **Sun, 2006**. Also, Magnetite NPs have been used extensively in the forward osmosis (FO) process, after being coated with a proper surfactant, due to the merit of magnetic recovery which lowers the cost of the process, **Ling, 2012**. Moreover, the production model of this nanomaterial make the scale-up process easy, **Alejo, et al., 2017**. Methods for preparing MNPs include thermal decomposition, microemulsion, and co- precipitation method. Some of these methods have been used to synthesize monodispersed MNPs, but precise control of size, shape, and surface of MNPs is generally challenging, **Medintz, et al., 2005**. On the other hand, producing large quantities of uniform-sized nanocrystals will be perilous because of the requirement of high quality nanosize in many nanotechnological applications. For example, the color sharpness of biomedical imaging probes and semiconductor optical devices based on nanocrystals strongly relies on the homogeneity of the nanocrystals, **Faraji, et al., 2010**.

As one convenient and cheap method, chemical co-precipitation has the potential to meet the growing demand for the direct production of good dispersed magnetite NPs. This method may be the simplest and most effective chemical path to obtain magnetic particles because it offers a low-temperature substitute to traditional powder synthesis techniques in the preparation of NPs, and the sizes of NPs can be well controlled by appropriate surface coating, Nidhin, et al., 2008. Chemical co-precipitation can yield high-purity, fine particles of single and multicomponent metal oxides, **Chen, et al., 2005**. The main feature of this process is that quantitative amount of NPs can be prepared. However, it has limited control on particle size distribution because the growth of the crystal is controlled only by kinetic elements, **Laurent, et al., 2008**. In the co-precipitation process, two stages are involved, **Gribanow, et al., 1990 and Cornell, and Schwertmann, 1996**: a rapid nucleation happens when the reactants concentration reaches to the critical supersaturation state, and

the second stage is slow growth of the nuclei by diffusion of the solute substances to the surface of the crystal. These two steps should be separated, in order to have monodisperse iron oxide NPs, i.e., nucleation should be averted during the growth period, **Tartaj, et al., 2006**. Iron oxides (Fe_3O_4 or γ-Fe_2O_3) are usually prepared by an aging stoichiometric mixture of ferric and ferrous salts in alkaline medium and the chemical reaction of the formation of magnetite (Fe_3O_4) can be written as in Eq. (1), **Laurent, et al., 2008**.

$$Fe^{2+} + 2Fe^{3+} + 8OH^- \longrightarrow Fe_3O_4 + 4H_2O \quad (1)$$

The thermodynamics of this reaction expect complete precipitation of Fe_3O_4 at a pH value in the range 8 to 14, with a molar ratio of 1:2 (Fe^{2+}/ Fe^{3+}) in an environment free of oxygen, **Jolivet, et al., 2004**. However, magnetite (Fe_3O_4) is vulnerable to oxidation because it is not very stable. It can transform to maghemite (γ-Fe_2O_3) in the presence of oxygen, **Laurent, et al., 2008**.

Iron oxide NPs have the characteristic of large surface-to-volume ratio and therefore they own high surface energies. As a result, they have the tendency to agglomerate so as to reduce their surface energies, **Na, et al., 2014**. Moreover, the bare MNPs have high chemical activity and are easy to be oxidized in the presence of oxygen (especially magnetite), resulting in loss of magnetism and dispersibility. Hence, it is essential to develop an active protection strategy to maintain the stability of these NPs by providing appropriate surfactant, such as polymers, **Wu, et al., 2008**. Also, the aggregation of small crystallites during synthesis leads to the formation of larger particles sizes, **Ocana, et al., 1995**.

The zeta (ζ) potential is the electrostatic potential at the boundary dividing the compact layer and the diffuse layer of the colloidal particles, **Ostolska, and Wisniewska, 2014**. It is a measure of the stability of NP suspensions. The higher electric charge on the surface of the NPs the more they will be safe from being agglomerated in buffer solution and that ensures easy redispersion because of the strong repulsive forces among particles, **Honary, and Zahir, 2013**. As a rule of thumb, absolute zeta potential values over 30 mV give good stability and over 60 mV excellent stability, while about 20 mV sustain only short-term stability. Values in the range -5 mV to +5 mV indicate fast aggregation, **Al-Kazazz, et al., 2016**.

The synthesis of uniform-sized, monodisperse nanoparticles is of key importance because the characteristics of these NPs depend intensely on their measurements, **Goldstein, et al., 1992**. From the fundamental scientific perspective, it is very important to control sizes of nanocrystals to characterize the size-dependent physical properties of them, **Steigerwald, and Brus, 1990**. The magnetic properties of NPs depend on their size. When the size of iron oxide NPs becomes smaller than 20 nm they are classified as superparamagnetic materials, i.e., they have no coercivity and no remanent magnetization when the external magnetic field is removed. Above this limit of size, the MNPs are ferri-/ferromagnetic materials that stay magnetized after the removal of the magnet, **Baumgartner, et al., 2013**.

The first controlled preparation of superparamagnetic iron oxide particles using alkaline precipitation of ferric and ferrous ions was achieved by, **Massart, 1981**. The key to control the sizes of the NPs is to adjust the rivalry between nucleation and growth. When the nucleation ratio is larger than growth ratio of seeds, the sizes of MNPs will be smaller or else the sizes will be larger,

Hui, et al., 2008. The size and shape of the nanoparticles can be affected by many factors including pH, temperature, nature of the salts (perchlorates, chlorides, sulfates, and nitrates), the Fe^{2+}/Fe^{3+} molar ratio, mixing rate, injection flux and the presence of oxygen, **Babes, et al., 1999**. The particle mean size of magnetite is intensely dependent upon the acidity degree of the precipitation medium, **Vayssie`res, et al., 1998 and Jiang, et al., 2004**. The higher the pH of the medium, the smaller the particle size and the more narrow size distribution will be, because this factor controls the chemical structure of the crystal surface and hence the electrostatic surface charge of the particles, **Tartaj, et al., 2006**. The size of MNPs is also decreased with the increase of the reaction temperature suggesting there is better polydispersity in the reaction at higher temperatures because increasing the reaction temperature would minimize the degree of agglomeration of magnetite nucleus and reduce sizes of their particles, **Mahdavi, et al., 2013**. A reasonable explanation for this is that by increasing temperature, more energy will be added within the solution leading to increasing motion which resulted in increasing the number of collisions among the particles, **Mahdavi, et al., 2011**. Several other researchers reported the same conclusion about the significance of using elevated temperature in reducing MNPs size, **Gribanow, et al., 1990, Babes, et al., 1999 and Sun, and Zeng, 2002**.

Another important factor affecting the composition, size, morphology, and magnetic properties of co-precipitated NPs is the Fe^{2+}/Fe^{3+} ratio. Uniform size and composition of magnetite NPs is obtained at Fe^{2+}/Fe^{3+} ratio = 0.5, as reported by, **Babes, et al., 1999**, which is the same ratio used in the present work. An increase in the mixing rate leads to decrease in the particle size, **Faraji, et al., 2010**. This can be explained as when the mixing rate increased, the energy conveyed to the solution medium also increased and the reaction solution dispersed into smaller size droplets, **Sun, et al., 2006**. In the same way, when the base is added to the reactants a decrease in size as well as the polydispersity was noted as compared to the reverse process, **Faraji, et al., 2010.** While, injection flux rates do not seem to have a predominant influence on the nanoparticle synthesis, **Babes, et al., 1999**. Bubbling inert gas through the solution or conduct the process of synthesis under the protection of inert gas not only protects magnetite from being oxidized but also reduces the particle size as compared to methods without inert gas protection, **Kim, et al., 2001, Gupta, and Wells, 2004, and Khan, 2008**.

In the present work, MNPs have been synthesized by two different methods with different parameters to study the effect of those parameters on the NP size. In the first method, nitrogen gas was used and reactants were added to the base during the synthesis process, while N_2 was not used in the second method and the base was added to the reactants. Also, the temperature of the process was high in the second method, and it was low (room temperature) in the first. Both MNPs were characterized by XRD, AFM, SEM and zeta potential. Also, nitrogen was used as the inert gas only to deoxygenate the distilled water used to dissolve iron salts, and the influence of using nitrogen in that way on the particle size was studied beside other parameters.

2. MATERIALS AND METHODS

Magnetic nanoparticles were synthesized by the co-precipitation of ferric and ferrous ions in alkaline medium following two methods. The synthesis processes were conducted in the chemical engineering department/ University of Baghdad. In the first method, 0.85 ml of 12 M HCl (37% concentration, from ROMIL-SA) and 25 ml of distilled water (produced by GFL - Gesellschaft für Labortechnik water distillation unit, Germany) deoxygenated by bubbling N_2 gas for 30 minutes were mixed, and 5.2 g of $FeCl_3$ (from Sinopharm Chemical) and 4.448 g of $FeSO_4 \cdot 7H_2O$ (from

BDH Chemicals, England), which represents 1:2 (Fe^{2+}/Fe^{3+}) molar ratio, were consecutively dissolved in the solution with stirring. The resulting solution was added dropwise into 250 ml of 1.5 M NaOH (99% purity from Applichem GmbH, Germany) solution with vigorous mixing (600 rpm) at room temperature. The pH value of the reaction environment was 14. The last step produced an instant black precipitate of Fe_3O_4. The reaction is fast and magnetite NPs can be seen instantly after adding iron salts. The paramagnetic was tested in-situ by putting a magnet near the black precipitate as shown in **Fig. 1**. The precipitate was isolated in the magnetic field of the magnet, and the supernatant liquid was removed by decantation with distilled water several times until the pH of the solution is neutral. To obtain the MNPs in a powdered form, the precipitant was isolated from the solution and dried in a dryer at 50℃ for 4 h and then overnight at room temperature. Thus, MNPs-1 were obtained.

In the second method, MNP-2 were synthesized as follows. 6.5 g of $FeCl_3$ and 5.56 g of $FeSO_4.7H_2O$, which also represents 1:2 (Fe^{2+}/Fe^{3+}) molar ratio, were dissolved in 50 ml of 0.5 M HCl solution. Then, 500 ml of 1.5 M NaOH was added dropwise to the solution under vigorous mixing (600 rpm) with heating at 80℃. The pH value of the reaction environment was also 14. The rest of the preparation steps are the same as in the first method. It is essential to understand the physicochemical characteristics of the prepared nanoparticles to comprehend their performance in the application they are used for. Therefore, the prepared MNPs have been characterized by X-ray diffractometer, XRD (SHIMADZU X-RAY DIFFRACTOMETER/ Lab X/ XRD 6000, Japan, scan range: 10.0000 - 120.0000 deg) to confirm the magnetite phase. The zeta-potential of the MNPs was measured with Zeta potential Analyzer (Zeta Plus, Brookhaven-USA with zeta potential range : -150 to + 150 mV) to understand the extent of stability of MNPs, and they were imaged using scanning electron microscope, SEM (Model: Tescan VEGA 3 SB). Atomic force microscope, AFM (SPM-AA3000 Angstrom Advanced Inc., Scanning Probe Microscope, USA) was used to determine the average particle size of MNPs and the particle size distribution.

3. RESULTS AND DISCUSSION

The preparation of MNPs by co-precipitation method is a well-known and widely used process. **Fig. 2** shows XRD patterns of MNPs-1 and MNPs-2. Both patterns demonstrate a highly crystalline structure for Fe_3O_4. The characteristic peaks of magnetite observed in the XRD pattern of 30.1, 35.4, 43.1, 53.5, 57 and 62.7˚ for MNPs-1, and 30.3, 35.7, 43.4, 53.8, 57.3 and 62.9˚ for MNPs-2 correspond to the diffractions of 220, 311, 400, 422, 511 and 440˚ crystal faces of Fe_3O_4 spinel structure, respectively. These results are in good consistency with the XRD patterns of magnetite nanoparticles reported by, **Hui, et al., 2008**. Scherrer's equation was used to determine crystallite size of MNPs:

$$D = \frac{K*\lambda}{\beta*COS\theta} \quad (2)$$

Where: D is the mean size of the crystallite (nm), K is the shape factor of the crystallite (dimensionless), λ is the x-ray wavelength (nm), β is the line broadening at half the maximum intensity (FWHM) (radians), and θ is the x-ray diffraction angle (degrees).

According to Scherrer's equation and using FWHM values of the most intense peaks obtained from XRD, the obtained crystallite size of MNPs-1 and MNPs-2 are 14.3 nm and 13.8 nm, respectively. The surface charges of the MNP-1 and MNPs-2 were measured by zeta potential analysis. The results show that they have zeta potential values of 2.77 mV and -12.48 mV, respectively. This means that MNPs-2 is more stable than MNPs-1 and the latter aggregates faster because of the lower absolute zeta potential value it possesses. Therefore, MNPs-1 has larger particle size because of the fast aggregation, even though the difference in size is small. **Fig. 3** shows graphs of zeta potential. Also, both types of MNPs were imaged with SEM as shown in **Fig. 4**. Atomic Force Microscope, AFM was also used to characterize MNPs. AFM results show particle size of 86.01 nm and 74.14 nm for MNPs-1 and MNPs-2, respectively, which is consistent with the results of zeta potential and XRD. **Fig. 5** shows AFM images and **Fig. 6** shows the particle size distribution of MNPs. In the synthesis of MNPs-1, nitrogen gas was used in a limited way. In other words, the process was not completely purged with nitrogen gas which means that the factor of using inert gas during synthesis of MNPs is not completely applied here. This could explain why the obtained particle size of MNPs-1 is larger than the particle size of MNPs-2.

Finally, by comparing MNPs-1 and MNPs-2, many synthesizing factors were found to be different including using N_2 gas, temperature, and adding a base to the reactants, while other factors are similar, such as pH, Fe^{2+}/Fe^{3+} molar ratio, and mixing rate. As a result, larger size MNPs-1 than MNPs-2 were obtained with a small difference. Although N_2 gas was used in the first method, it was not used to protect the atmosphere of the reaction, its use was in a limited way and not through purging the process. All the different factors used in the two synthesis processes including using N_2, temperature and adding a base to the reactants, support the obtained results. As for pH, Fe^{+2}/Fe^{+3} molar ratio, and mixing rate, they were similar in both methods despite their effect on the results. All the aforementioned factors of the synthesis of MNPs-1 and MNPs-2 is summarized in **Table 1**.

4. CONCLUSIONS

In this work, MNPs, which can be used in many applications (such as biomedical, water treatment, industrial and information storage field), were synthesized by co-precipitation method at two different conditions. In the first method, MNPs with particle size 86.01 nm was obtained from synthesis conditions 25℃, Fe^{2+}/Fe^{3+} molar ratio equal to 0.5, pH=14, mixing rate 600 rpm, the N_2 gas used for deoxygenating of the water used for dissolving iron salts, and with the addition of reactants to the base. In the second method, MNPs with particle size 74.14 nm was obtained from synthesis conditions 80 ℃, no N_2 gas was used, the addition of base to the reactants with the similar remaining factors. XRD characterization proved the formation of magnetite phase with crystallite size 14.34 and 13.84 nm for MNPs-1 and MNPs-2, respectively. Zeta potential analysis showed that MNPs-2 is more stable than MNPs-1 with zeta potential values -12.48 and 2.77 mV, respectively.

5. REFERENCES

- Alejo, T., Arruebo, M., Carcelen, V., Monsalvo, V. M. and Sebastian, V., 2017, *Advances in Draw Solutes for Forward Osmosis: Hybrid Organic-Inorganic Nanoparticles and Conventional Solutes*, Chemical Engineering Journal, Vol. 309, PP. 738–752.
- Al-Kazazz, F. F., Al-Hakeim, H. K. and Al-Aobaid, H. K., 2016, *Study the Interaction Between LH, FSH, and TSH with New Synthesized Magnetic Nanoparticles Coated with Dextran*, Medical Journal of Babylon, Vol. 13, PP. 421 - 434.
- Babes, L., Denizot, B., Tanguy, G., Le Jeune, J. J. and Jallet, P., 1999, *Synthesis of Iron Oxide Nanoparticles Used as MRI Contrast Agents: A Parametric Study*, Journal of Colloid and Interface Science, Vol. 212, PP. 474-482.
- Baumgartner, J., Bertinetti, L., Widdrat, M., Hirt, A. M. and Faivre, D., 2013, *Formation of Magnetite Nanoparticles at Low Temperature: from Superparamagnetic to Stable Single Domain Particles*, PLOS ONE, Vol. 8. https://doi.org/10.1371/journal.pone.0057070
- Bucak, S., Yavuztürk, B., and Sezer, A. D., 2012, *Magnetic Nanoparticles: Synthesis, Surface Modifications and Application in Drug Delivery*, InTech, http://dx.doi.org/10.5772/52115.
- Chen, S., Feng, J., Guo, X., Hong, J. and Ding, W., 2005, *One-Step Wet Chemistry for Preparation of Magnetite Nanorods*, Materials Letters, Vol. 59, PP. 985–988.
- Cornell, R. M., Schwertmann, U., 1996, *The Iron Oxides: Structure, Properties, Reactions, Occurrence and Uses*, VCH: Weinheim.
- Faraji, M., Yamini, Y. and Rezaee, M., 2010, *Magnetic Nanoparticles: Synthesis, Stabilization, Functionalization, Characterization, and Applications*, Journal of The Iranian Chemical Society, Vol. 7, PP. 1-37.
- Goldstein, A. N., Echer, C. M. and Alivisatos, A. P., 1992, *Melting in Semiconductor Nanocrystals*, Science, Vol. 256, PP. 1425-1427.
- Gribanow, N. M., Bibik, E. E., Buzunov, O. V. and Naumov, V. N., 1990, *Physico-Chemical Regularities of Obtaining Highly Dispersed Magnetite by the Method Of Chemical Condensation*, Journal of Magnetism and Magnetic Materials, Vol. 85, PP. 7-10.
- Gupta, A. K., and Wells, S., 2004, *Surface-Modified Superparamagnetic Nanoparticles for Drug Delivery: Preparation, Characterization, and Cytotoxicity Studies*, IEEE Transactions on Nanobioscience, Vol. 3, PP. 66-73.
- Honary, S. and Zahir, F., 2013, *Effect of Zeta Potential on the Properties of Nano-Drug*, Journal of Pharmaceutical Research, Vol. 12, PP. 265-273.
- Hong, R. Y., Li, J. H., Li, H. Z., Ding, J., Zheng, Y. and Wei, D. G., 2008, *Synthesis of Fe_3O_4 Nanoparticles Without Inert Gas Protection Used as Precursors Of Magnetic Fluids*, Journal of Magnetism and Magnetic Materials, Vol. 320, PP. 1605–1614.
- Hui, C., Shen, C., Yang, T., Bao, L., Tian, J., Ding, H., Li, C.and Gao, H. -J., 2008, *Large-Scale Fe_3O_4 Nanoparticles Soluble in Water Synthesized by a Facile Method*, Journal of Physical Chemistry C, Vol. 112, PP. 11336–11339.

- Hyeon, T., 2003, *Chemical Synthesis of Magnetic Nanoparticles*, Chemical Communications, Vol. 8, PP. 927-934.
- Jiang, W., Yang, H. -C., Yang, S. Y., Horng, H. E., Hung, J. C., Chen, Y. C. and Hong, C. -Y., 2004, *Preparation and Properties of Superparamagnetic Nanoparticles with Narrow Size Distribution and Biocompatible*, Journal of Magnetism and Magnetic Materials, Vol. 283, PP. 210-214.
- Jolivet, J.-P., Chaneac, C. and Tronc, E., 2004, *Iron Oxide Chemistry. from Molecular Clusters to Extended Solid Networks*,Chemical Communication, Vol. 5, PP. 481-487.
- Khan, A., 2008, *Preparation and Characterization of Magnetic Nanoparticles Embedded in Microgels*, Materials Letters, Vol. 62, PP. 898–902.
- Kim, D. K., Zhang, Y., Voit, W., Rao, K. V. and Muhammed, M. J., 2001, *Synthesis and Characterization of Surfactant-coated Superparamagnetic Monodispersed Iron Oxide Nanoparticles*, Journal of Magnetism and Magnetic Materials, Vol. 225, PP.30-36.
- Laurent, S., Forge, D., Port, M., Roch, A., Robic, C., Elst, L. V. and Muller, R. N., 2008, *Magnetic Iron Oxide Nanoparticles: Synthesis, Stabilization, Vectorization, Physicochemical Characterizations, and Biological Applications*, Chemical Reviews, Vol. 108, PP. 2064–2110.
- Ling. M. M., 2012, *Integration of Nanoparticles as Draw Solute in Forward Osmosis*, Ph.D. Thesis, National University of Singapore.
- Mahdavi, M., Ahmad, M. B., Haron, M. J. and Ab Rahman, M. Z., 2011, *Optimized Conditions for Graft Copolymerization of Polyacrylamide onto Rubberwood Fibre*, BioResources, Vol. 6, PP. 5110–5120.
- Mahdavi, M., Ahmad, M. B., Haron, M. J., Namvar, F., Nadi, B., Ab Rahman, M. Z. and Amin, J., 2013, *Synthesis, Surface Modification and Characterisation of Biocompatible Magnetic Iron Oxide Nanoparticles for Biomedical Applications*, Molecules, Vol. 18, PP. 7533-7548.
- Massart, R., 1981, *Preparation of Aqueous Magnetic Liquids in Alkaline and Acidic Media*, IEEE Transactions on Magnetics, Vol. 17, PP. 1247-1248.
- Medintz, I. L., Uyeda, H. T., Goldman, E. R. and Mattoussi, H., 2005, *Quantum Dot Bioconjugates for Imaging, Labelling and Sensing*, Nature Materials, Vol. 4, PP. 435-446.
- Na, Y., Yang, S. and Lee. S., 2014, *Evaluation of Citrate-Coated Magnetic Nanoparticles as Draw Solute for Forward Osmosis*, Desalination, Vol. 347, PP. 34–42.
- Nidhin, M., Indumathy, R, Sreeram, K. J. and Nair, B. U., 2008, *Synthesis of Iron Oxide Nanoparticles of Narrow Size Distribution on Polysaccharide Templates*, Bulletin of Materials Science, Vol. 31, PP. 93–96.
- Ocana, M., Rodriguez-clemente, R. and Serna, C. J., 1995, *Uniform Colloidal Particles in Solution-Formation Mechanisms*, Advanced Materials, Vol. 7, PP. 212–216.
- Ostolska, I. and Wiśniewska, M., 2014, *Application of the Zeta Potential Measurements to Explanation of Colloidal Cr_2O_3 Stability Mechanism in the Presence of the Ionic Polyamino Acids*, Colloid and Polymer Science, Vol. 292, PP. 2453-2464.

- Steigerwald, M. L. and Brus, L. E., 1990, *Semiconductor Crystallites: a Class of Large Molecules*, Accounts of Chemical Research, Vol. 23, PP. 183-188.
- Sun, J., Zhou, S., Hou, P., Yang, Y., Weng, J., Li, X. and Li, M, 2006, *Synthesis and Characterization of Biocompatible Fe_3O_4 Nanoparticles*, Journal of Biomedical Materials Research, Part. A, Vol. 10, PP. 333–341.
- Sun, S. and Zeng, H., 2002, *Size-Controlled Synthesis of Magnetite Nanoparticles*, Journal of the American Chemical Society, Vol. 124, PP. 8204-8205.
- Sun, S. H., 2006, *Recent Advances In Chemical Synthesis, Self-Assembly, and Applications of FePt Nanoparticles*, Advanced Materials, Vol. 18, PP.393-403.
- Tartaj, P., Morales, M. P., Veintemillas-Verdaguer, S., Gonzalez- Carreno, T. and Serna, C. J., 2006, *Synthesis, Properties and Biomedical Applications of Magnetic Nanoparticles*, Handbook of Magnetic Materials, Vol. 16, PP. 403-482.
- Vayssie`res, L., Chane´ac, C., Tronc, E. and Jolivet, J. –P,1998, *Size Tailoring of Magnetite Particles Formed by Aqueous Precipitation: An Example of Thermodynamic Stability of Nanometric Oxide Particles*, Journal of Colloid and Interface Science, Vol. 205, PP. 205-212.
- Wu, W., He, Q. G. and Jiang, C. Z., 2008, *Magnetic Iron Oxide Nanoparticles: Synthesis and Surface Functionalization Strategies*, Nanoscale Research Letters, Vol. 3, PP. 397–415.

NOMENCLATURE

D	mean size of the crystallite, nm
β	line broadening at half the maximum intensity (FWHM), radians
θ	x-ray diffraction angle, degrees
K	the shape factor of the crystallite, dimensionless
λ	x-ray wavelength, nm

ABBREVIATIONS

MNPs	Magnetic nanoparticles
XRD	X-ray diffractometer
AFM	atomic force microscope
SEM	scanning electron microscope
NPs	Nanoparticles
FO	Forward osmosis
MRI	Magnetic resonance imaging
MNPs-1	Magnetic nanoparticles produced from the first method
MNPs-2	Magnetic nanoparticles produced from the second method
fcc	face-centered cubic
T_d	Tetrahedral
O_h	Octahedral

Table 1. Parameters of two methods of synthesis of MNPs.

Parameter	**MNPs-1**	**MNPs-2**
pH	14	14
Temperature	25℃	80℃
Fe^{2+}/Fe^{3+} molar ratio	0.5	0.5
Mixing rate	600 rpm	600 rpm
Adding base to the reactants	reactants added to the base	base added to the reactants
Using N_2 gas	N_2 gas was used in limited way (only for deoxygenation of water used to dissolve iron salts.	no N_2 gas was used
Nanoparticle size	86.01 nm	74.14 nm

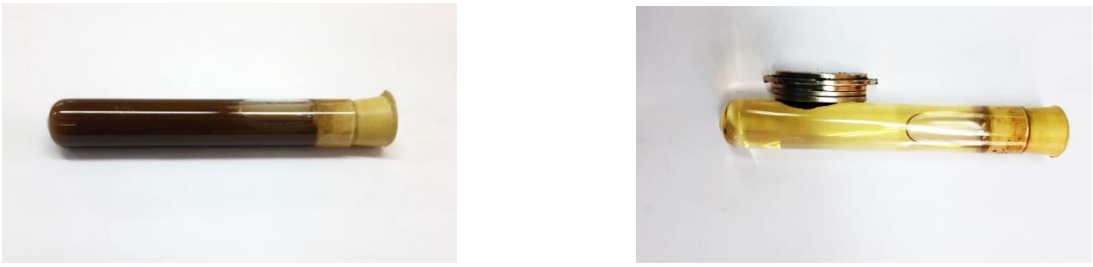

(a) **(b)**

Figure 1. MNPs solution (a) before placing a magnet (b) after placing a magnet, where the MNPs can be seen isolated in the magnetic field.

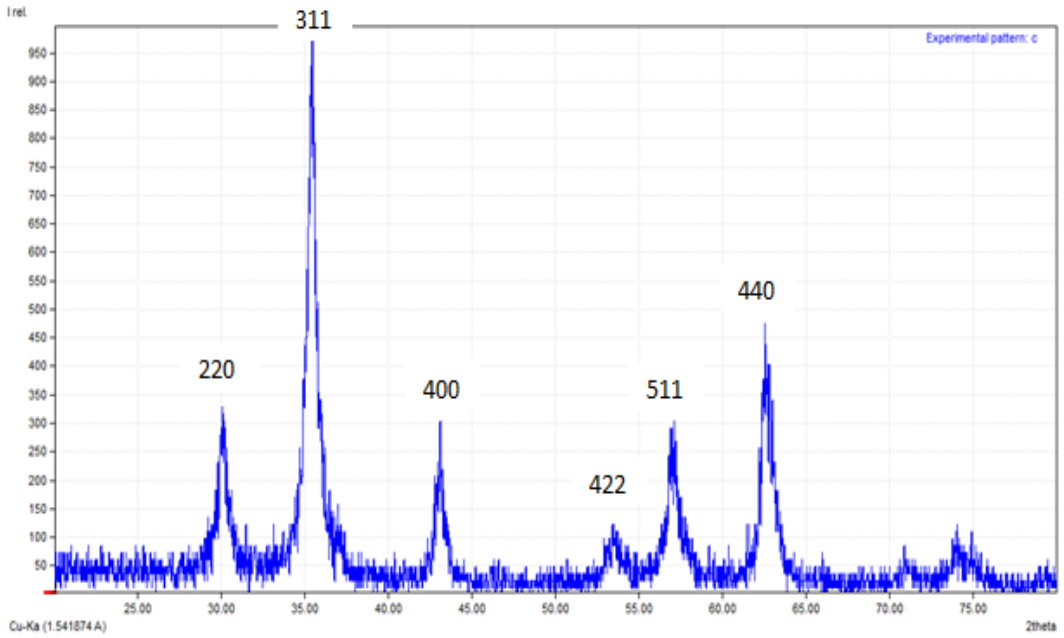

(a)

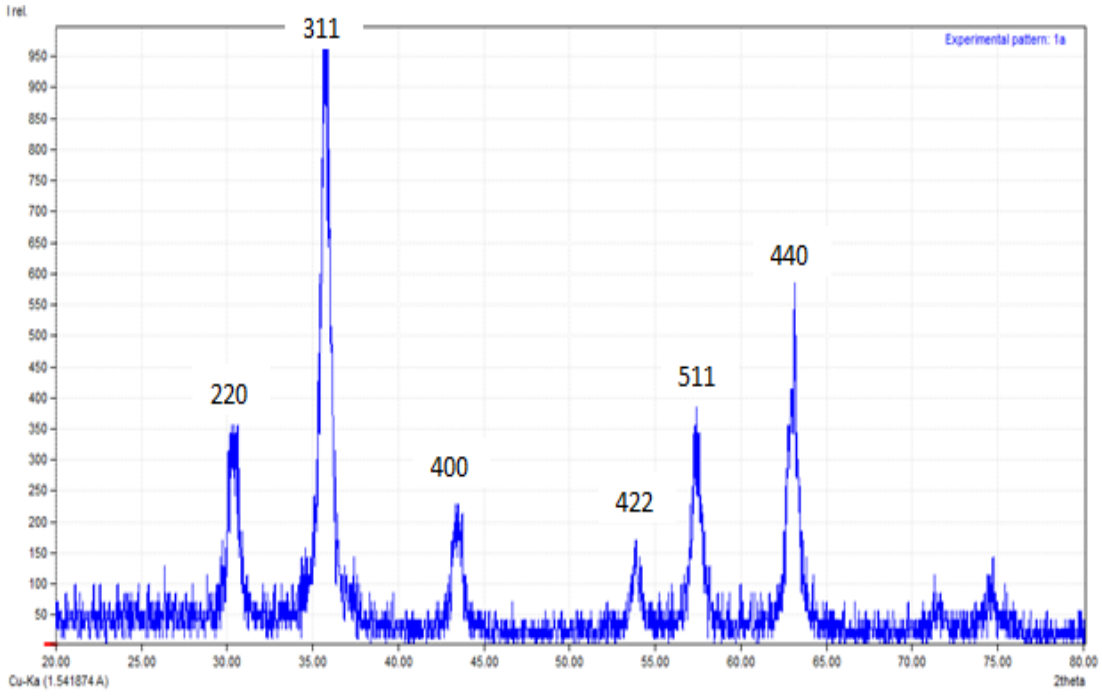

(b)

Figure 2. XRD patterns of (a) MNPs-1 and (b) MNPs-2.

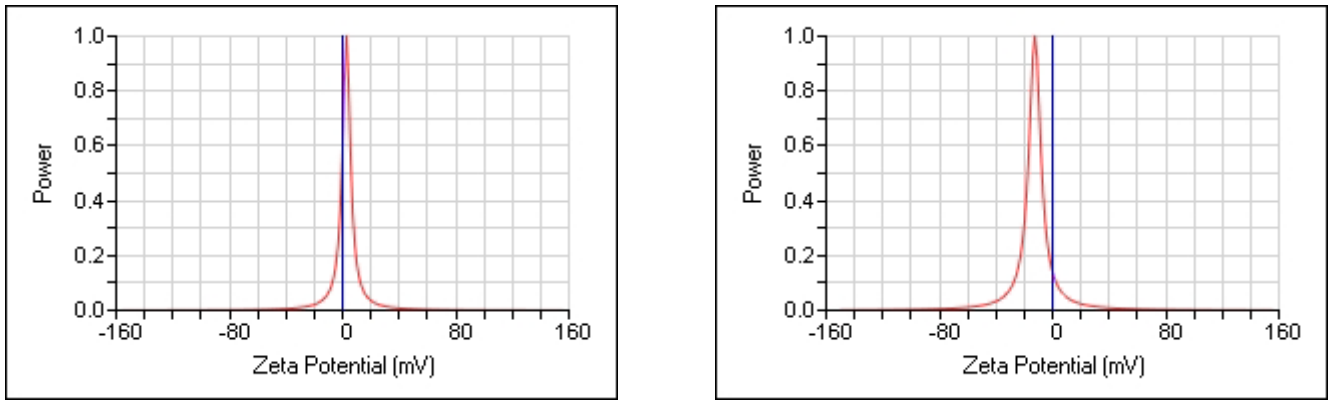

(a) (b)

Figure 3. Zeta potential of (a) MNPs-1 and (b) MNPs-2.

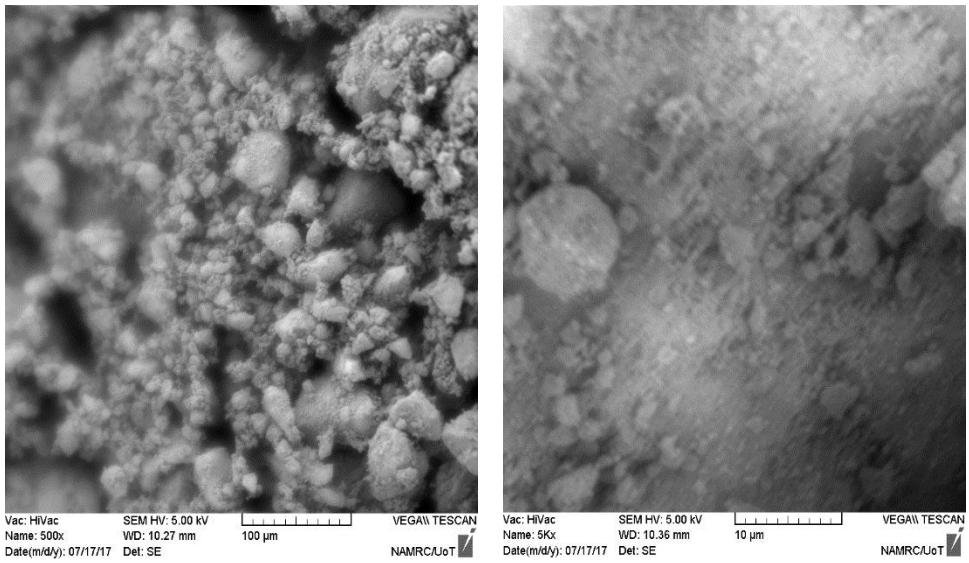

(a) (b)

Figure 4. SEM images of (a) MNPs-1 and (b) MNPs-2.

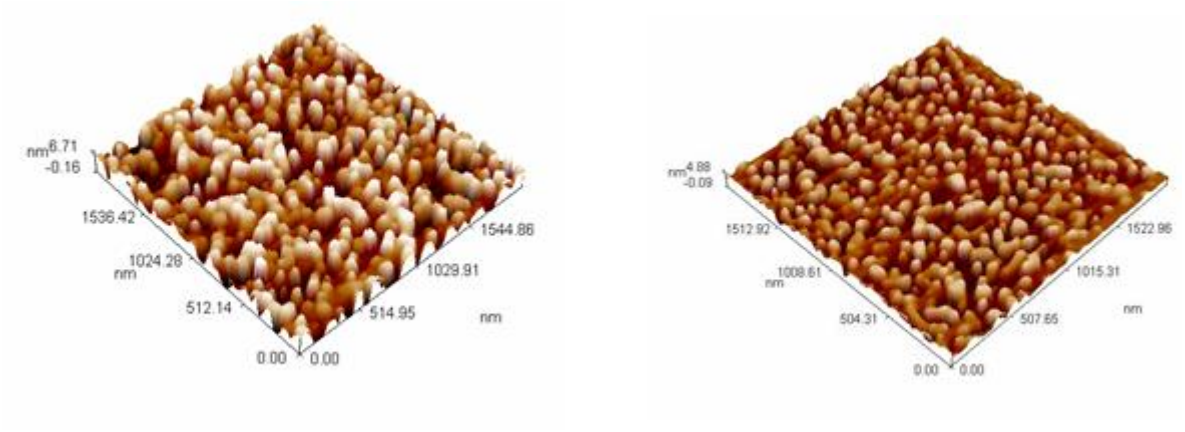

(a) (b)

Figure 5. AFM images of (a) MNPs-1 and (b) MNPs-2.

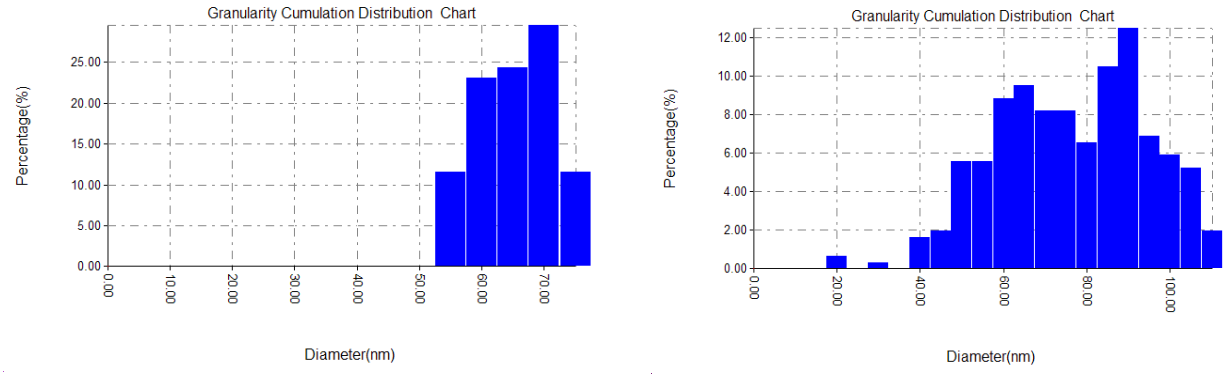

(a) (b)

Figure 6. Particle size distribution of (a) MNPs-1 and (b) MNPs-2.